Magneto-optical spectrum of donors in $Al_xGa_{1-x}As$ and its implications on the *DX* center

T. Inoshita*
Fundamental Research Laboratories, NEC Corporation, 4-1-1 Miyazaki, Miyamae-ku, Kawasaki, Kanagawa 213, Japan

N. Iwata
Microelectronics Research Laboratories, NEC Corporation, 4-1-1 Miyazaki, Miyamae-ku, Kawasaki, Kanagawa 213, Japan
(Received 6 July 1989; revised manuscript received 20 February 1990)

The $1s$-$2p$ intracenter optical transitions of shallow donors in n-type $Al_xGa_{1-x}As$ ($x=0.18$ and 0.24) were investigated by far-infrared photoconductivity in magnetic fields of up to 10 T. The spectra could be well fitted by the hydrogenic effective-mass model, and were analyzed in terms of the effective mass m^* and the linewidth. The result indicates (1) the inadequacy of the usual linear interpolation scheme for $m^*(x)$ and (2) the importance of alloy disorder in line broadening. No evidence was seen for the interaction of the shallow-donor ground state with the *DX* center, which is inconsistent with the model based on the *DX* center being an A_1 state with small lattice relaxation.

I. INTRODUCTION

The nearly perfect lattice matching of $Al_xGa_{1-x}As$ with GaAs makes it the most important class of semiconductor mixed crystal, used extensively as a buffer layer in various heterostructures and quantum confined systems. This situation has led to substantial improvement in the growth techniques of $Al_xGa_{1-x}As$, such as molecular-beam epitaxy (MBE). Epitaxial films are now available with sufficient purity to allow detailed investigation of the electronic structure of shallow impurities contained therein.

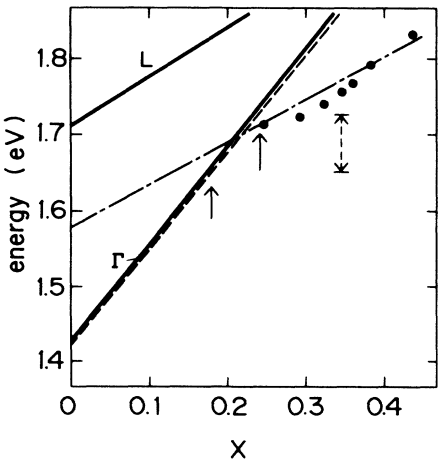

FIG. 1. Energy positions of the Γ and L conduction-band minima (solid lines) and the hydrogenic donor ground state associated with the Γ minimum (dashed line) in $Al_xGa_{1-x}As$. The circles denote the *DX* levels obtained from Hall measurements (Ref. 12), and the dash-dotted line is their free extrapolation as quoted in Ref. 7. The Al content x of the samples used in the present study is indicated by solid arrows, and the energy separation (~80 meV) between the donor ground states of the two samples is shown by the dashed arrow.

The electronic structure of donors in $Al_xGa_{1-x}As$ is interesting for several reasons. First, it provides a unique way to evaluate material parameters such as the conduction-band effective mass, which is difficult to obtain by transport studies due to poor mobility. Second, the alloy disorder inherent in mixed crystals is expected to more or less affect the donor spectrum.[1] The effect of alloy disorder on localized states is a subject not yet fully explored.[2,3] Third, a deep level called a *DX* center, known for its peculiar properties (such as persistent photoconductivity and a large barrier for trapping as well as emission) is known to exist in n-type $Al_xGa_{1-x}As$.[4-7] Its origin has recently been a matter of debate. For $x<0.2$, the *DX* state is located in the conduction-band continuum as a resonant state.[8-11] Hall measurements have indicated that its energy decreases as x increases, and for $x>0.2$ the state comes into the band gap as a deep state (Fig. 1).[12] Thus a crossover takes place between the donor and the *DX* levels at $x\cong 0.2$. This proximity of the donor and the *DX* levels suggests the possibility of gaining insight into the symmetry of the *DX* state by seeing whether or not there is interaction between the two.

In the present work, the electronic structure of the shallow donor in $Al_xGa_{1-x}As$ with $x\sim 0.2$ is investigated by far-infrared photoconductivity using magnetic fields of up to 10 T with the purpose of investigating the aforementioned problems. After presenting the experimental methods in Sec. II, the results and discussions are given in four parts in Sec. III: The first part, which describes the general features of the spectra, is followed by three fairly independent parts devoted, respectively, to the analysis of the effective mass, the peak broadening, and the implications on the *DX* center. A summary is given in Sec. IV.

II. EXPERIMENTAL

The mode of far-infrared photoconductivity measurement we applied to $Al_xGa_{1-x}As$ is the so-called photothermal ionization spectroscopy.[13,14] In this method,

high-purity n-type (or p-type) semiconductors are kept at temperatures low enough for the conduction electrons to freeze out on the donor ground states. If the sample is illuminated by far-infrared light, each electron is excited first to a higher donor level by absorption of a photon, and subsequently to the conduction band by absorption of phonons. (In order for such phonons to be available, the temperature should not be excessively low.) The resulting photoconductivity spectrum consists of sharp lines at energies equal to the separation between the ground state and various (mainly $2p$) excited states. The process involves both photons and phonons: hence the name "photothermal."

The measurements were made using a Digilab FTS-20E rapid-scan Michelson interferometer. The light emitted from a mercury lamp is introduced into the interferometer with the moving mirror scanned at a constant velocity. The output light, whose intensity is temporally modulated, is conducted down into a cryostat through a light pipe. The sample is placed at the end of the light pipe with its surface perpendicular to the pipe. The sample resistance as a function of time is Fourier transformed to obtain the spectrum. This raw spectrum is subsequently divided by the spectrum of the impinging light to get the final spectrum. The sample temperature was set equal to 4.2 K for magnetic fields $B < 6$ T, whereas for $B > 6$ T it was increased to ~ 10 K to improve signal-to-noise ratio.

The cryostat is equipped with a superconducting solenoid with the solenoid axis parallel to the pipe and, therefore, perpendicular to the sample surface (Faraday configuration). More details about the apparatus are found in Ref. 15.

As for the samples, we used two epitaxial films of $Al_xGa_{1-x}As$ with $x = 0.18$ and 0.24, respectively, grown by MBE on semi-insulating GaAs(100) substrates. The $x = 0.18$ sample (No. 1A) consists of an undoped GaAs buffer layer (3000 Å thick), undoped $Al_{0.18}Ga_{0.82}As$ buffer layer (5000 Å thick), and a Si-doped $Al_{0.18}Ga_{0.82}As$ layer (2 μm thick) grown successively. The sample with $x = 0.24$ (No. 2A) is structured as an undoped GaAs layer (4000 Å thick), an undoped $Al_xGa_{1-x}As$ graded layer (1000 Å thick) with x varying linearly from 0 to 0.24, and an undoped $Al_{0.24}Ga_{0.76}As$ layer (6000 Å thick) (all acting as a buffer) followed by a Si-doped $Al_{0.24}Ga_{0.76}As$ layer (3 μm thick). Contacts to the samples were made by Sn alloying. For comparison reasons, we also studied two n-type GaAs samples: one sample (No. 1B) is comparable to the $Al_xGa_{1-x}As$ samples in impurity concentration, whereas the other sample (No. 2B) is of very high purity. The electrical characteristics of these samples are tabulated in Table I.

The Al composition x of $Al_xGa_{1-x}As$ was obtained by x-ray diffraction with the substrate-induced strain taken into account. The resulting values of x agree with the values obtained from photoluminescence measurements to the digits quoted.

III. RESULTS AND DISCUSSIONS

A. General features of the spectrum

The photoconductivity spectra for sample No. 1A at $B = 0$, 5, and 10 T are shown in Fig. 2. As seen from the figure, a magnetic field splits the dominant peak at $B = 0$ into two; the higher peak moves rapidly to higher energy, whereas the lower peak is rather insensitive to B. This trend is typical of $1s$-$2p(\pm)$ transitions. This is more clearly seen in Fig. 3(a), which presents the variation of the peak wave number with B. The peak positions agree well with the $1s$-$2p(\pm)$ transition energies in the hydrogenic effective-mass model with a suitable choice of the effective mass and the dielectric constant. (No plotting is made in the range $0 < B < 4$ T, where the two peaks overlap and could not successfully be separated by Gaussian or Lorentzian fitting.) No evidence was seen for the interaction of the donor states with other localized states. (Such interaction would manifest itself as an anticrossing behavior.) A similar plot for sample No. 2A is shown in Fig. 3(b). Again the validity of the hydrogenic model is clear.

It is also seen from Fig. 2 that the widths of the $2p(\pm)$ peaks are rather large and depend little on B, in strong contrast with the rapid decrease in the peak width with B commonly seen in GaAs.[14] More detailed discussions on this point will be given in Sec. III C.

B. Electron effective mass

In the hydrogenic effective-mass model, the energy separation Δ between the $2p(+)$ and $2p(-)$ states can be expressed as[16]

$$\Delta = \frac{e\hbar}{m^* c} B \ . \tag{1}$$

In practical units, it can be written as

TABLE I. Electrical characteristics of the samples derived from Hall measurements. (Here N_D and N_A denote donor and acceptor concentrations, respectively, K is the compensation ratio N_A/N_D, and μ is the electron mobility.)

Sample No.	x	N_d-N_A (cm^{-3})	K	$\mu_{77\,K}$ (cm^2/V sec)
1A	0.18	6.9×10^{15}		7 700
2A	0.24	9.5×10^{15}		4 500
1B	0	5.5×10^{15}	0.3	28 000
2B	0	$<5\times10^{13}$	<0.4	180 000

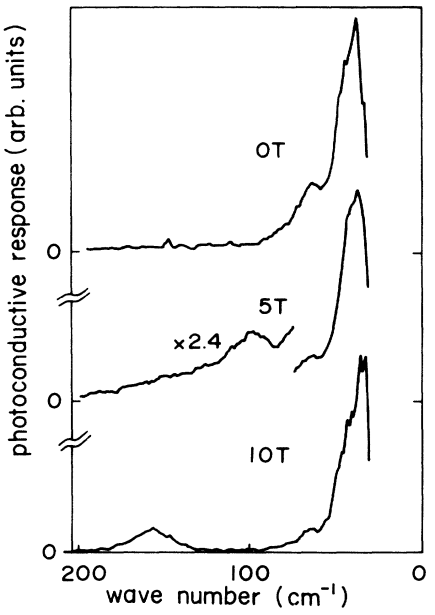

FIG. 2. Photoconductive response of sample No. 1A at different magnetic-field strengths taken with a resolution of 2 cm^{-1}.

$$\Delta\ (cm^{-1}) = \frac{0.9339}{m^*/m_0} B\ (T)\ , \tag{1'}$$

where m_0 is the free-electron mass. Thus m^* can be obtained from the slope of Δ versus B.

Figure 4 presents the plot of the difference between the experimental $1s$-$2p(+)$ and $1s$-$2p(-)$ peak energies against B. From a least-squares fitting, we deduce $m^*/m_0 = 0.0767$ and 0.0774 for $x = 0.18$ and 0.24, respectively. In the literature, it is usually assumed, without any justification, that m^* goes linearly with x,[17]

$$m^*/m_0 = 0.067 + 0.083x\ . \tag{2}$$

The B dependence of Δ for the two samples assuming Eq. (2) is shown in Fig. 4 by the dashed lines. It clearly shows the inadequacy of the linear interpolation.

An alternative form for $m^*(x)$,

$$m^*/m_0 = \left[\frac{x}{0.14} + \frac{1-x}{0.067} \right]^{-1}\ , \tag{3}$$

has been suggested by Harrison and Hauser,[18] who provided a plausibility argument for Eq. (3) on the basis of the effective-mass theory and the virtual-crystal approximation. The experimental values of m^* for sample Nos. 1A and 2A together with that for GaAs sample No. 1B are compared with Eqs. (2) and (3) in Fig. 5, which shows that Eq. (3) agrees fairly well with the experiment.

Let us now discuss the validity of Eq. (1). Since Eq. (1) involves only the excited states, it is free from central cell corrections, which are important only for the ground state.[19] As for nonparabolicity, it is important only for strong fields such that $\hbar\omega_c$ (cyclotron energy) $\gg E_g$ (band gap), which is equivalent to $\gamma = \hbar^3\varepsilon^2 B/m^{*2}ce^3 \gg 1$.[20] ($\gamma$ is equal to $\hbar\omega_c$ divided by twice the effective Rydberg.) In our experimental situation, $\gamma < 1$, which justifies the neglect of nonparabolicity.

The Stark effect of random static electric fields, produced by ionized donors and acceptors, has been investigated by Stillman *et al.*[16] For very high purity n-type GaAs ($N_D = 5.2\times10^{13}$ cm^{-3}, $N_A = 2.2\times10^{13}$ cm^{-3}), they have shown that the Stark effect indeed causes deviation from Eq. (1) for $B < 0.5$ T, the mass obtained from Eq. (1)

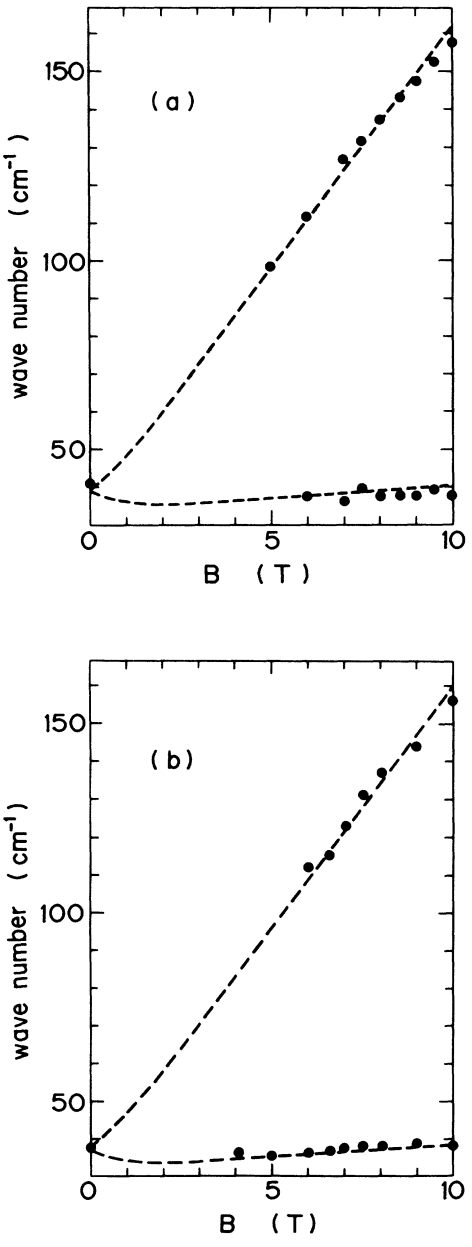

FIG. 3. Energy of the $1s$-$2p(+)$ (higher-energy) and $1s$-$2p(-)$ (lower-energy) peaks vs magnetic field for (a) sample No. 1A and (b) sample No. 2A. The dashed curves present least-squares fitting by the hydrogenic effective-mass model.

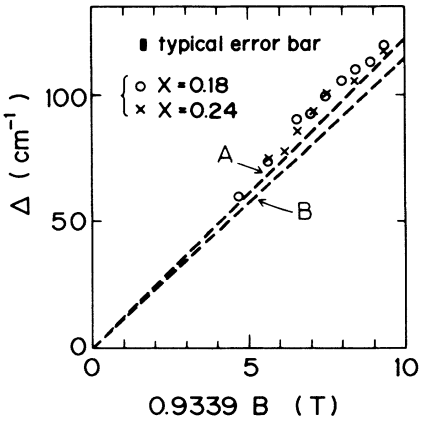

FIG. 4. Experimental energy separation Δ between $2p(+)$ and $2p(-)$ levels of $Al_xGa_{1-x}As$ vs magnetic field B. The dashed lines denote the hydrogenic theory using linear interpolation for $m^*(x)$. (A and B correspond to $x=0.18$ and 0.24, respectively.)

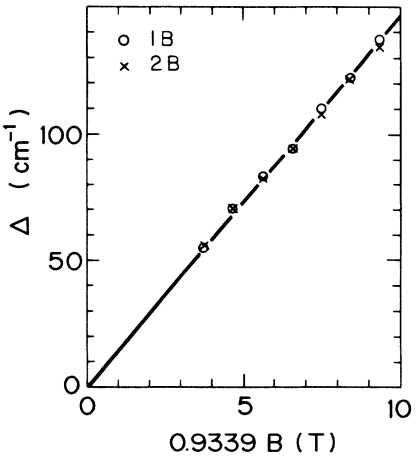

FIG. 6. Experimental energy separation between $2p(-)$ and $2p(+)$ levels of the two GaAs samples vs B. The line denotes the hydrogenic effective-mass model with $m^*/m_0=0.068$.

underestimating the real value. The effect was found to be negligible for higher fields $B>1$ T. Since these authors used samples of substantially higher purity than ours, direct application of their result to our case requires some caution, and we should check the impurity concentration dependence of the effect. This can be done by comparing the spectra for the two GaAs samples: with higher impurity concentration (sample No. 1B) and with lower impurity concentration (sample No. 2B). Figure 6 presents the plot of Δ versus B for the two. Good agreement is seen in the range of the magnetic field studied ($B>4$ T). This leads to the conclusion that the Stark effect is also negligible in our analysis of m^* for $Al_xGa_{1-x}As$, which is done for $B>5$ T. This result for GaAs further indicates that the overlap between donors does not give any appreciable correction to Eq. (1) either, in the impurity concentration range we are considering here.

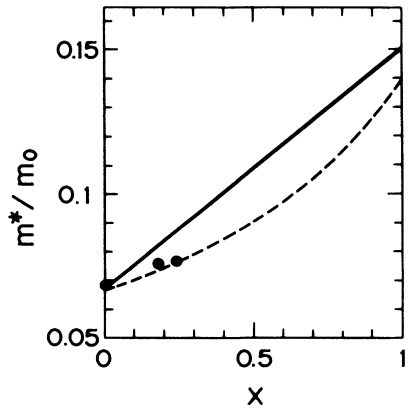

FIG. 5. Experimental values of m^* (circles), the linear interpolation formula (solid line), and Harrison's formula [Eq. (3)] (dashed line).

Another mechanism that might possibly affect Eq. (1) is the random-alloy potential (RAP). The effect of the long-wavelength part of the RAP (i.e., composition fluctuation with a size greater than a_B, where a_B is the effective Bohr radius for the donor) has been studied theoretically in Ref. 1 for the case $B=0$. The result indicates that the peaks in the $2p(\pm)$ density of states shift only slightly upward, an order of magnitude smaller than the shift of $1s$. (If we use τ_{1s}, calculated in Sec. III C, in Fig. 2 of Ref. 1, the resulting shift of $2p(\pm)$ is only 0.3 cm^{-1}.) Further, the shift is the same for $2p(+)$ and $2p(-)$, leaving Δ unaffected. When $B\neq 0$, the shifts should no longer be the same for the two states, but the shifts themselves are likely to decrease with B, since magnetic fields bring the levels farther apart reducing the coupling (by the RAP) between $2p(\pm)$ and other levels.

As for the shorter-range part of the RAP, no theory has been worked out yet as to its effect on donors. Thus we cannot fully rule out the possibility of its affecting Eq. (1). However, the effect is expected to be small, since the shift they produce should be smaller for excited states than for the ground state. Further, the preceding argument for the long-range part [i.e., that the shifts of $2p(+)$ and $2p(-)$ are nearly equal, leaving Δ unchanged, and B would tend to reduce the effect] should apply also to the short-range part. Thus the use of Eq. (1) in our analysis seems well justified.

Having derived m^*, we can make a least-squares fit of the experimental peak energies [$1s$-$2p(\pm)$ transition energies as functions of B] with ε as the only fitting parameter. The result is shown by dashed curves in Figs. 3(a) and 3(b). [Optimal values of ε turned out to be 12.67 for $x=0.18$ and 12.97 for $x=0.24$. These values should not be taken too seriously, since the fitting involves the ground state ($1s$), for which central cell corrections may be important. This is in strong contrast with the case of m^*, which is free from central cell corrections.]

C. Linewidth

In GaAs with modest impurity concentration, the $1s$-$2p$ linewidth arises from the Stark and quadrupolar broadening mechanisms[16,21] (i.e., broadening due to electric field and field gradients produced by ionized impurities) and from donor-donor overlaps. It is interesting to compare the peak widths of $Al_xGa_{1-x}As$ (Fig. 2) with GaAs of comparable impurity concentration (sample No. 1B).

Figure 7 presents the magnetic-field dependence of the full width at half maximum (FWHM) of the $1s$-$2p(+)$ peaks of sample Nos. 1A (crosses) and 1B (circles). In the case of sample No 1B, the width decreases with B from 16 cm^{-1} at $B=0$ to 10 cm^{-1} at $B=10$ T. This decrease results from magnetic-field-induced shrinkage of the donor wave function, which reduces donor overlaps, and the Stark and quadrupolar broadening. [The Stark broadening is proportional to d^3, whereas the quadrupolar broadening goes as d^4, where d is a typical dimension of the charge distribution of donor $2p(+)$ orbital.[21] Thus, the broadening in these mechanisms is a rapidly decreasing function of B.] In sample No. 1A, in contrast, the peak width, aside from being twice as large as that of sample 1B, is fairly constant with B, with perhaps a very slight decrease. This suggests that, although donor-donor overlaps and Stark (quadrupolar) effects are not negligible, there is also another mechanism at work that gives a larger width for a larger B.

The most likely mechanism for this additional broadening is RAP. In the absence of magnetic fields, the width of the $2p$ density of states due to the long-wavelength part of RAP is an order of magnitude smaller than that of the $1s$ state.[1] Thus the RAP broadening of the $1s$-$2p$ transition is approximately equal to the width of the $1s$ state γ_{1s}, which can be expressed as[1]

$$\gamma_{1s}^2=(dE_c/dx)^2x(1-x)/(4\pi Na_B^3)\ . \tag{4}$$

Here N is the concentration of the group III lattice sites,

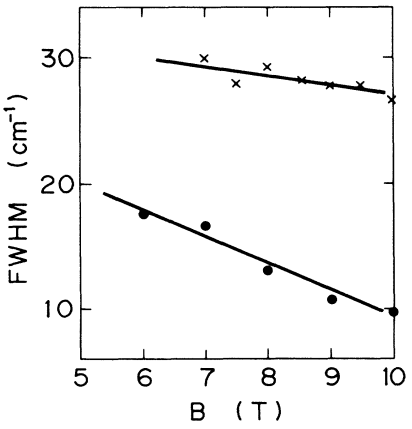

FIG. 7. The full width at half maximum (FWHM) of the $1s$-$2p(+)$ peak of sample Nos. 1A (crosses) and 1B (circles) vs B.

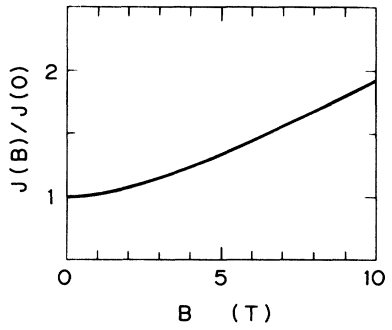

FIG. 8. $J=\int\phi^4d^3r$, where ϕ is the donor ground-state envelope function, calculated as a function of B. The calculation was done by the hydrogenic effective-mass approximation and the finite-element method, using m^* and ε appropriate for sample No. 1A.

and E_c denotes the energy of the Γ conduction-band minimum as a function of x. Using E_c from Ref. 22, the calculated FWHM of $2p(\pm)$ peaks for our samples is approximately 8 cm^{-1}, which compares fairly well with the difference in the widths of sample Nos. 1A and 1B (Fig. 7). Although the authors of Ref. 1 have not explicitly treated the case $B\neq0$, it is easy to see that the width in this mechanism is proportional to $J=\int\phi^4d^3r$ even when $B\neq0$, where ϕ is the ground-state envelope function. Assuming the hydrogenic model for the donor, we calculated J numerically using for ϕ the ground-state wave function of a hydrogen atom in a magnetic field, which is obtained again numerically by the finite-element method.[23,24] The value thus calculated was scaled with m^* and ε for sample No. 1A obtained in Sec. III B. Figure 8 presents $J(B)$ normalized to its value at $B=0$. It is seen that J increases by 90% as B increases from 0 to 10 T. This is in remarkably good agreement with the increase in the separation between the plots of sample Nos. 1A and 1B in Fig. 7.

No theory has thus far been worked out regarding the effect of the shorter-range part of the RAP on the donor spectrum. Although one would intuitively feel that such an effect is less important than the long-range part, the problem still remains open.

The lifetime broadening is usually negligibly small. For example, the lifetime τ of the $2p(\pm)$ states of n-type GaAs (N_D-N_A in the lower 10^{14} cm^{-3} range) has been measured.[24] The obtained τ is approximately 50 nsec and 500 nsec for the $2p(+)$ and $2p(-)$ states, respectively, at $B=0$. This translates into linewidth ($=\hbar/\tau$) of the order of only 10^{-4} cm^{-1} and 10^{-5} cm^{-1}, respectively, which are at least five orders of magnitude smaller than the broadening seen in our $Al_xGa_{1-x}As$ samples. It is quite doubtful that the larger impurity concentration or some alloy-specific effect, if any, in our samples brings about such an enormous enhancement of the linewidth.

D. Implications on the *DX* center

As was mentioned in the Introduction, the ground state of the *DX* center, as obtained by Hall-effect mea-

surements, lies very close (to within ~40 meV) to the donor ground state in the range of x studied here (Fig. 1). One expects that this proximity gives rise to interaction (anticrossing) between the DX and shallow-donor states provided they are of the same symmetry. In the preceding sections we have seen that the donor $1s$-$2p(\pm)$ transitions are well accounted for by the hydrogenic model, with no evidence for anticrossing. This experimental finding has an important consequence on the origin of the DX center, as will be shown below.

The DX center was originally supposed to be a composite defect consisting of a simple donor and an unknown defect, hence the name "DX."[6] Since then, numerous studies have appeared that point to the inadequacy of this model, and now there is a near consensus that DX is an isolated substitutional donor.[7] The DX center models proposed to date can be classified into the following three categories: (i) one-electron (positive-U) models with small lattice relaxation (SLR),[25–28] (ii) one-electron models with large lattice relaxation (LLR),[29–33] and (iii) a two-electron (negative-U) model with large lattice relaxation.[34] There has been an active debate concerning the correct model of the DX center, especially the amount of lattice relaxation. Despite experiments to settle the argument, no clear-cut consensus has been reached. For example, Mooney *et al.*[32] found no detectable photoionization cross section for DX below 0.8 eV, supporting LLR. Henning and Ansems,[35] on the other hand, found a finite cross section down to 0.2 eV, which is in contradiction with LLR and favors SLR. In this section, we will investigate the SLR models and see if they are consistent with our experimental results.

The first SLR model proposed was that by Hjalmarson and Drummond,[25] who simply assumed that the DX center is a donor with a deep s-like ground state and a shallow first excited state that is also s like. In this work, the mechanism that drives the ground state deep is not specified. Subsequently, Yamaguchi made a Green's-function calculation (with a tight-binding basis) of the electronic structure of a substitutional donor in $Al_xGa_{1-x}As$ (without lattice distortion).[26] The result indicated that the central cell potential causes substantial deepening of the A_1 symmetric ground state, which he identified with the DX level. Henning and Ansems,[27] in an attempt to fit their photoluminescence data, proposed a SLR model in which DX is identified with a donor state associated with the L minima. (Their model is rather complex, but the remaining details are not important here.) Finally, Bourgoin and Mauger[28] proposed that DX is the donor ground state of A_1 symmetry, associated with the L minima, which is deepened by intervalley mixing effects.

It is important to note that, in the Henning-Ansems model and in the Bourgoin-Mauger model, the DX level (assumed to be associated with the L minima) is distinct from the donor ground state associated with the Γ minimum [hereafter denoted as $1s(\Gamma)$]. In the Hjalmarson-Drummond and Yamaguchi models, on the other hand, it is unclear if DX and $1s(\Gamma)$ are distinct. (The Green's-function method used by Yamaguchi has so far been successful only for deep levels but does not give shallow states. Thus the method does not lend itself to any discussion of the relation between deep and shallow states. In the case of the Hjalmarson-Drummond model, the authors avoid specifying if the deep donor state they refer to derives from a Γ-associated donor level or from some other state, such as an L-associated donor level.)

Experimental evidence that DX and $1s(\Gamma)$ are distinct (but arise from the same center) has been provided by a far-infrared absorption study of direct gap $Al_xGa_{1-x}As$ carried out by Theis *et al.*[36] This is also consistent with the fact that we have observed hydrogenic (unperturbed) $1s$-$2p$ transitions for $0<B<10$ T at $x=0.24$ (where the DX level should be well below the Γ minimum). Thus we assume that DX and $1s(\Gamma)$ are distinct levels. Accepting further that the DX center is an isolated substitutional donor,[7] the shallow ground state Φ_s and the DX state Φ_d can be obtained as eigenstates of the same Hamiltonian $H_0+U(r)$, where H_0 is the perfect crystal Hamiltonian and $U(r)$ presents the change in the potential caused by the introduction of the donor. [Strictly speaking, the impurity potential $U(r)$ differs slightly for the two states due to different valence charge distributions. This difference should be negligible for the crude estimation given below.]

The energies E of the shallow-donor state and the DX state are obtained by solving the secular equation[37]

$$\begin{vmatrix} E_s-E & V \\ V^* & E_d-E \end{vmatrix}=0 . \tag{5}$$

Here E_s and E_d are the unperturbed energies of the shallow and DX states, respectively, and the interaction matrix V can be expressed as

$$V=\int \Phi_s^* U \Phi_d d^3r . \tag{6}$$

As for U, we used the pseudopotential for a Si substitutional donor in GaAs obtained from a Green's-function calculation within the local-density functional scheme.[38] (The nonlocal part of U was neglected.)

The Φ_s was taken to be

$$\Phi_s=\phi_g\psi_\Gamma , \tag{7}$$

where $\psi_\Gamma(\mathbf{r})$ is the Bloch function (pseudowavefunction) at the Γ point for bulk GaAs (Ref. 39) obtained by using the same Green's-function scheme as was used for U. As for the envelope function $\phi_g(\mathbf{r})$, we used the ground-state wave function of the hydrogen atom with its mass and the dielectric constant replaced by m^* and ε, respectively, obtained for sample No. 1A in Sec. III B. (We need only consider the ground state, since, by symmetry, the $2p$ states do not interact with an A_1 state even in the presence of a magnetic field.) The DX center was modeled as

$$\Phi_d=\tilde{\phi}_{1s}\left[\sum \psi_L/4\right] , \tag{8}$$

where ψ_L is the L-point Bloch function, the summation is over the four inequivalent L points, and

$$\tilde{\phi}_{1s}(r;b)=(b^3\pi)^{-1/2}e^{-r/b}$$

is the hydrogenic $1s$ function with its radius b taken as a parameter. (As seen from Fig. 1, the DX energy level roughly follows the L valley as x varies, suggesting that DX has a strong L character.)

We are mainly interested in the extent to which the shallow-donor energy as a function of magnetic field B is affected by the proximity of the DX level. Since the DX center is highly localized, its energy E_d as well as the wave function Φ_d should be nearly independent of B. This allows us to neglect their magnetic-field dependence. Then the magnetic-field dependence of E derives from E_s, as well as from ϕ_g in Φ_s. The function ϕ_g cannot be obtained analytically when $B \neq 0$ and was numerically calculated by the finite-element method.[23] (The energies obtained in this method for hydrogen $1s$ and $2p$ states in the range $\gamma < 1$ agree with the values given in Ref. 40 to within 10^{-3} Ry.)

Figure 9 presents the calculated V as a function of b for $B = 0$ and 10 T. Although $|V|$ decreases rapidly with b, it remains quite large, at least on the order of the donor effective Rydberg, in the realistic range of b. Figure 9 also reveals that V depends only weakly on B.

There are also claims that the DX center has an appreciable Γ character aside from L.[38] Thus we also calculated V using

$$\Phi_d = \tilde{\phi}_{1s}\psi_\Gamma \ , \tag{8'}$$

instead of Eq. (8). The result, shown by the dashed curves in Fig. 9, is not much different from that obtained from Eq. (8), indicating that V is quite insensitive to the detailed form of Φ_d. (We have also tried using Bloch functions, corresponding to various different points in the Brillouin zone, in Φ_d and found the result to be insensitive to these choices. Thus our conclusion is valid even if Φ_d is an admixture of all points in the Brillouin zone.[33,34]

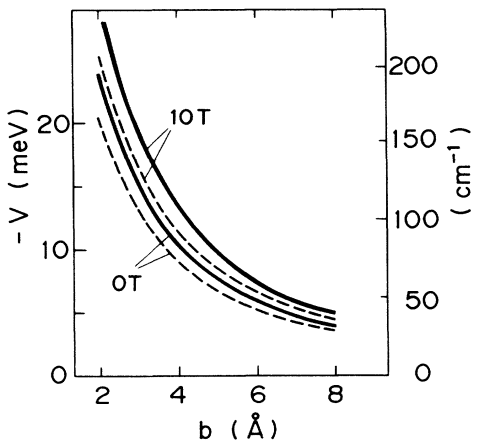

FIG. 9. Calculated interaction matrix element V as a function of the DX center radius b for different magnetic-field strengths. The solid curves represent the case $\Phi_d = \tilde{\phi}_{1s}\left[\sum \psi_L/\sqrt{4}\right]$, and the dashed curves denote the case $\Phi_d = \tilde{\phi}_{1s}\psi_\Gamma$.

Using the obtained value of V in Eq. (5), we have the energy of the impurity levels with their mutual interaction taken into account. A typical result is shown in Fig. 10. In deriving this result, we used the hydrogenic donor spectrum, with m^* and ε pertinent to sample No. 1A, for E_s, and V was set equal to 40 cm^{-1} (=5 meV) (its magnetic-field dependence was neglected). The calculation was done for different values of E_d, which was taken as a parameter. (All the energies are taken relative to the Γ conduction-band minimum.)

As seen from Fig. 1, the DX level crosses the donor ground state at $x \sim 0.2$, i.e., between the x values of our two samples. It is also to be noted that the donor ground-state energies differ by 80 meV for the two samples (dashed arrow in Fig. 1). Thus the DX level should lie within less than about 40 meV (=320 cm^{-1}) from the donor ground state in at least one of the samples. Figure 10 shows that if model (i) were correct, we would observe a significant shift in the $1s$ level in at least one of the samples. (The $1s$ level would shift upward for $x = 0.24$ and downward for $x = 0.18$.) The calculated shift is as large as 5 cm^{-1} even when $E_d = 300$ cm^{-1}; for such a large shift, the spectrum can no longer be fit by the hydrogenic model. The fact that no such anomaly was seen constitutes strong evidence against the small relaxation A_1 model for the DX center.

We have also estimated the interaction between the donor $2p(\pm)$ states and the DX center, assuming that the latter is of T_2 symmetry. The impurity wave functions were modeled by replacing the $1s$-type envelope functions

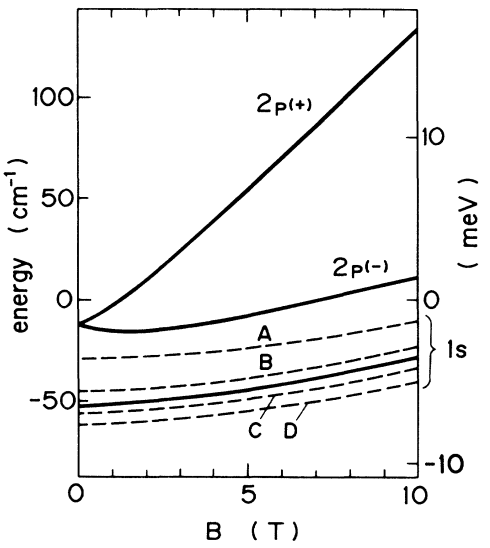

FIG. 10. Solid lines represent the unperturbed hydrogenic spectrum of the shallow donor in $Al_{0.18}Ga_{0.82}As$ calculated using m^* and ε determined for sample No. 1A. The dashed lines are the energy of the donor ground state obtained by solving Eq. (5) for different values of E_d: $E_d = -100$ cm^{-1} (A), -300 cm^{-1} (B), 300 cm^{-1} (C), and 100 cm^{-1} (D). The zero of energy is taken to be the conduction-band bottom in the absence of a magnetic field.

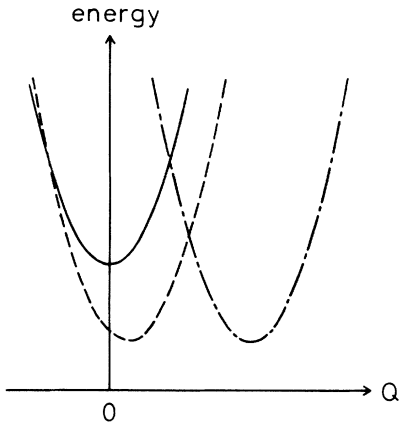

FIG. 11. Schematic configuration coordinate diagrams for small lattice relaxation (dashed line) and large lattice relaxation (dash-dotted line) for the *DX* state. The solid line denotes the conduction-band bottom.

in Eqs. (7) and (8) by corresponding $2p(\pm)$ functions. The resulting V was found to be three orders of magnitude smaller than in the case of the $1s$-A_1 interaction. (This is because both Φ_s and Φ_d are vanishingly small near the impurity site where U is large.) Such small interaction is impossible to detect by the present method. Thus our analysis cannot rule out the small relaxation T_2 model.

The situation is completely different in model (ii) or (iii). If the lattice relaxation is large (schematically shown by the dash-dotted line in Fig. 11), we should include the phonon wave function overlap in V, which makes V proportional to e^{-S}, where S is the Huang-Rhys factor.[41] Since large lattice relaxation means $S \gg 1$, V is orders of magnitude smaller than in the case of small lattice relaxation. Therefore, model (ii) does not contradict our experiment.

This argument, based on the one-electron picture, does not apply directly to the negative U (two-electron) model. However, since the model includes large lattice relaxation as an essential ingredient, the situation is the same in that the interaction matrix is again proportional to $e^{-S} \ll 1$. Thus the model also survives our experiment.

IV. SUMMARY

We have performed far-infrared photoconductivity measurements on $Al_xGa_{1-x}As$ with $x \sim 0.2$ in magnetic fields of up to 10 T. The spectrum could be well fitted by the hydrogenic effective-mass model, which is rather remarkable considering the proximity of the donor ground state to the *DX* level.

Through a least-squares fitting of peak energies against magnetic field B, the conduction-band effective mass m^* was derived. It was revealed that $m^*(x)$ exhibits considerable bowing and does not obey the usually assumed linear interpolation formula. The large linewidth and its slow decrease with B were explained by random-alloy potential. Finally, a model calculation of the interaction between the shallow-donor ground state and the *DX* center was performed. It was shown that if the *DX* center were an A_1 state with small lattice relaxation, it would significantly perturb the donor ground state. The fact that there was no such perturbation observed presents strong evidence against this model.

ACKNOWLEDGMENTS

We are grateful to A. Oshiyama for providing the result of his Green's-function calculation on GaAs:Si, and to M. Mizuta for illuminating discussions. Thanks also go to Y. Nashimoto and N. Furuhata for kindly donating the samples.

*Present address: 28-5 Oyamacho, Shibuya-ku, Tokyo 151, Japan.

[1]I. Y. Yanchev and G. L. Bleris, Semicond. Sci. Technol. **3**, 1217 (1988).

[2]T. Baba, M. Mizuta, T. Fujisawa, J. Yoshino, and H. Kukimoto, Jpn. J. Appl. Phys. **28**, L298 (1989).

[3]L. Samuelson, S. Nilsson, Z.-G. Wang, and H. G. Grimmeiss, Phys. Rev. Lett. **53**, 1501 (1984).

[4]R. J. Nelson, Appl. Phys. Lett. **31**, 351 (1977).

[5]D. V. Lang and R. A. Logan, Phys. Rev. Lett. **39**, 365 (1977).

[6]D. V. Lang, R. A. Logan, and M. Jaros, Phys. Rev. B **19**, 1015 (1979).

[7]For a review, see T. N. Theis, Inst. Phys. Conf. Ser. **91**, 1 (1988); also **95**, 307 (1989).

[8]M. Mizuta, M. Tachikawa, H. Kukimoto, and S. Minomura, Jpn. J. Appl. Phys. **24**, L143 (1985).

[9]T. N. Theis, B. D. Parker, P. M. Solomon, and S. L. Wright, Appl. Phys. Lett. **49**, 1542 (1986).

[10]M. A. Fisher, A. R. Adams, and E. P. O'Reilly, Phys. Rev. Lett. **59**, 2341 (1987).

[11]D. K. Maude, J. C. Portal, L. Dmowski, T. Foster, J. Eaves, M. Nathan, M. Heiblum, J. J. Harris, and R. B. Beall, Phys. Rev. Lett. **59**, 815 (1987).

[12]N. Chand, T. Henderson, J. Klem, W. T. Masselink, R. Fischer, Y-C. Chang, and H. Morkoc, Phys. Rev. B **30**, 4481 (1984).

[13]Sh. M. Kogan and T. M. Lifshits, Phys. Status Solidi A **39**, 11 (1977).

[14]G. E. Stillman, C. M. Wolfe, and J. O. Dimmock, in *Semiconductors and Semimetals,* edited by R. K. Willardson and A. C. Beer (Academic, New York, 1977), Vol. 12, Chap. 4.

[15]N. Iwata and T. Inoshita, Appl. Phys. Lett. **50**, 1361 (1987).

[16]G. E. Stillman, D. M. Larsen, and G. M. Wolfe, Phys. Rev. Lett. **27**, 989 (1971).

[17]H. C. Casey, Jr. and M. B. Panish, *Heterostructure Lasers* (Academic, New York, 1978), Pt. B.

[18]J. W. Harrison and J. R. Hauser, J. Appl. Phys. **47**, 292 (1976).

[19]F. Bassani, G. Iadonisi, and B. Preziosi, Rep. Prog. Phys. **37**, 1099 (1974).

[20]W. Trzeciakowsky, M. Baj, S. Huant, and L.-C. Brunel, Phys. Rev. B **33**, 6846 (1986).

[21]D. M. Larsen, Phys. Rev. B **8**, 535 (1973).

[22]H. Kroemer, Surf. Sci. **174**, 299 (1986).

[23]G. Strang and G. Fix, *An Analysis of the Finite Element*

Method (Prentice-Hall, New Jersey, 1973).
[24]G. R. Allan, A. Black, C. R. Pidgeon, E. Gornik, W. Seidenbusch, and P. Colter, Phys. Rev. B **31**, 3560 (1985).
[25]H. P. Hjalmarson and T. J. Drummond, Appl. Phys. Lett. **48**, 656 (1986).
[26]E. Yamaguchi, Jpn. J. Appl. Phys. **25**, L643 (1986).
[27]J. C. M. Henning and J. P. M. Ansems, Semicond. Sci. Technol. **2**, 1 (1987).
[28]J. C. Bourgoin and A. Mauger, Appl. Phys. Lett. **53**, 749 (1988).
[29]K. L. I. Kobayashi, Y. Uchida, and H. Nakashima, Jpn. J. Appl. Phys. **24**, L928 (1985).
[30]A. Oshiyama and S. Ohnishi, Phys. Rev. B **33**, 4320 (1986).
[31]T. N. Morgan, Phys. Rev. B **34**, 2664 (1986).
[32]P. M. Mooney, G. A. Northrop, T. N. Morgan, and H. G. Grimmeiss, Phys. Rev. B **37**, 8298 (1988).
[33]H. P. Hjalmarson and T. J. Drummond, Phys. Rev. Lett. **60**, 2410 (1988).
[34]D. J. Chadi and K. J. Chang, Phys. Rev. Lett. **61**, 873 (1988).
[35]J. C. M. Henning and J. P. Ansems, Appl. Phys. A **44**, 245 (1987).
[36]T. N. Theis, T. F. Kuech, L. F. Palmateer, and P. M. Mooney, Inst. Phys. Conf. Ser. **74**, 241 (1985).
[37]See Ref. 19, Eq. (4.15).
[38]A. Oshiyama, *Proceedings of the 19th International Conference on the Physics of Semiconductors, Warsaw, 1988,* edited by W. Zawadzki (Institute of Physics, Polish Academy of Science, Warsaw, 1988), p. 1059; A. Oshiyama, *Proceedings of the 15th International Conference on Defects in Semiconductors, Budapest, 1988,* edited by G. Ferenczi (Trans Tech, Aedermannsdorf, Switzerland, 1989), p. 287.
[39]A. Oshiyama and M. Saito, J. Phys. Soc. Jpn. **56**, 2104 (1987).
[40]P. C. Makado and N. C. McGill, J. Phys. C **19**, 873 (1986).
[41]J. Bourgoin and M. Lannoo, *Point Defects in Semiconductors II: Experimental Aspects* (Springer-Verlag, New York, 1983).